

# Supplementary Information for: The history of ice-sheet retreat on North America during Termination 5: implications for the origin of the sea-level highstand during interglacial stage 11

## Contents of this file

This supporting information document contains Sections S1, six figures (S1 to S6) and two tables (Tab. S1–S2) referred to in this document and the main text.

## Section S1. Age Model Construction

We used the depth modeling routine *Undatable* (Lougheed & Obrochta, 2019) to create age-depth models for the Site U1302/3 stratigraphy spanning MIS 13–11 (520–340 ka) and MIS 6–1 (the past ~187 kyr) to reconstruct the history of LIS break-up during three deglaciations: Termination (T) 5, T2, and T1. *Undatable* was used for this purpose because it allowed us to create age models for these time intervals that factor in both the age and depth uncertainties of the chronological markers used to generate them (Tabs. S1–S2 & SI Files ‘Undatable\_input1.csv’ and ‘Undatable\_input2.csv’). The output of the modelling routine (Figs. S1–S2 & SI Files ‘Undatable\_output1.txt’ and ‘Undatable\_output2.txt’) generates conservative age-depth uncertainties for every age constraint inputted using bootstrapping and an estimate of sediment accumulation rate uncertainty (Lougheed & Obrochta, 2019), which we then used to compare our datasets to changes in orbital insolation.

The existing Site U1302/3 age model (Channell et al., 2012) was based on tandem fitting of its planktic  $\delta^{18}\text{O}$  and relative paleointensity (RPI) stratigraphies to reference curves: the LR04 benthic  $\delta^{18}\text{O}$  stack (Lisiecki & Raymo, 2005) and PISO-1500 RPI stack (Channell et al., 2009). The PISO-1500 RPI stack (1-kyr resolution) has since been superseded by the HINAPIS-1500 (0.5-kyr resolution), which was constructed by stacking North Atlantic RPI stratigraphies of the past ~1500 kyr (from Ocean Drilling Program Sites 983, 984, and IODP sites U1306 and U1304) on an LR04-based age model (Xuan et al., 2016). In this study, we update the MIS 13–11 age model (~508–341 ka) for the corresponding part of the Site U1302/3 stratigraphy by tuning its RPI record (Channell et al., 2012) to the HINAPIS-1500 stack using 14 tie points (Fig. S4). We also updated the Site U1302/3 age model for MIS 6–1 (spanning the past ~187 kyr) by aligning its planktic  $\delta^{18}\text{O}$  stratigraphy to: (1) the Greenland NorthGRIP (NGRIP) ice core air temperature proxy record (Fig. S3a–b; Dansgaard et al., 1982) on the Greenland ice core chronology (GICC05; Rasmussen et al., 2014) calendar age-scale (i.e., calendar ka before 1950 (b1950; hereinafter ka) = AD 2000 (b2k) minus 50 yr), or (2) the Iberian Margin Core MD95-2042 benthic  $\delta^{18}\text{O}$  stratigraphy on its Lisiecki & Stern (2016) age model (Fig. S3e–f). Given the relatively large age uncertainties associated with these older target curves ( $\pm \sim 1\text{--}2\text{-kyr}$  at  $1\sigma$ ), we did not convert MD95-2042 ages to calendar ages. We also established 11 ties for this time interval between the Site U1302/3 RPI stratigraphy and the

HINAPIS stack (Fig. S3c–d). The age model for HINAPIS-1500 stack was derived from benthic  $\delta^{18}\text{O}$ -based ties to the LR04 stack. We use an age uncertainty of  $\pm 2.2$  ka ( $1\sigma$ ), which is derived from summing errors in quadrature (the square-root of the linear sum of squares) of the published LR04 age uncertainty ( $\pm 2$  ka at  $1\sigma$ ; Lisiecki & Raymo, 2005) and a conservative estimate of the likely depth uncertainty involved in tying the HINAPIS-1500 stack to the LR04 (which we take to be 50% of LR04 age-model uncertainty). It is argued, based on radiocarbon-based age models for T1, that the use of a single global alignment target like the LR04 stack neglects regional differences in the timing of benthic  $\delta^{18}\text{O}$  change during terminations (e.g., Skinner & Shackleton, 2005; Stern et al., 2014; Lisiecki & Stern, 2016), but also that the ages assigned to the LR04 for the past  $\sim 1.5$  Myr may be  $\sim 1$ – $2$ -kyr younger than they should be (Lisiecki & Stern, 2016). We have not used the LR04 to constrain the deglacial portions of our Site U1302/3 records for T2 and T1. While, the age model of the target curve (HINAPIS-1500) we have used to assign ages to MIS 12–11 records is underpinned by LR04 ages, based on T1, at least, no discernable differences are likely to exist in the timing of changes in benthic  $\delta^{18}\text{O}$  data during terminations in North Atlantic records when compared on their LR04 and independent radiocarbon-based stratigraphies (Lisiecki & Stern, 2016). Even if the ages we have assigned to our MIS 12/11 are  $\sim 1$ – $2$  kyr too young this would not change the findings we present here.

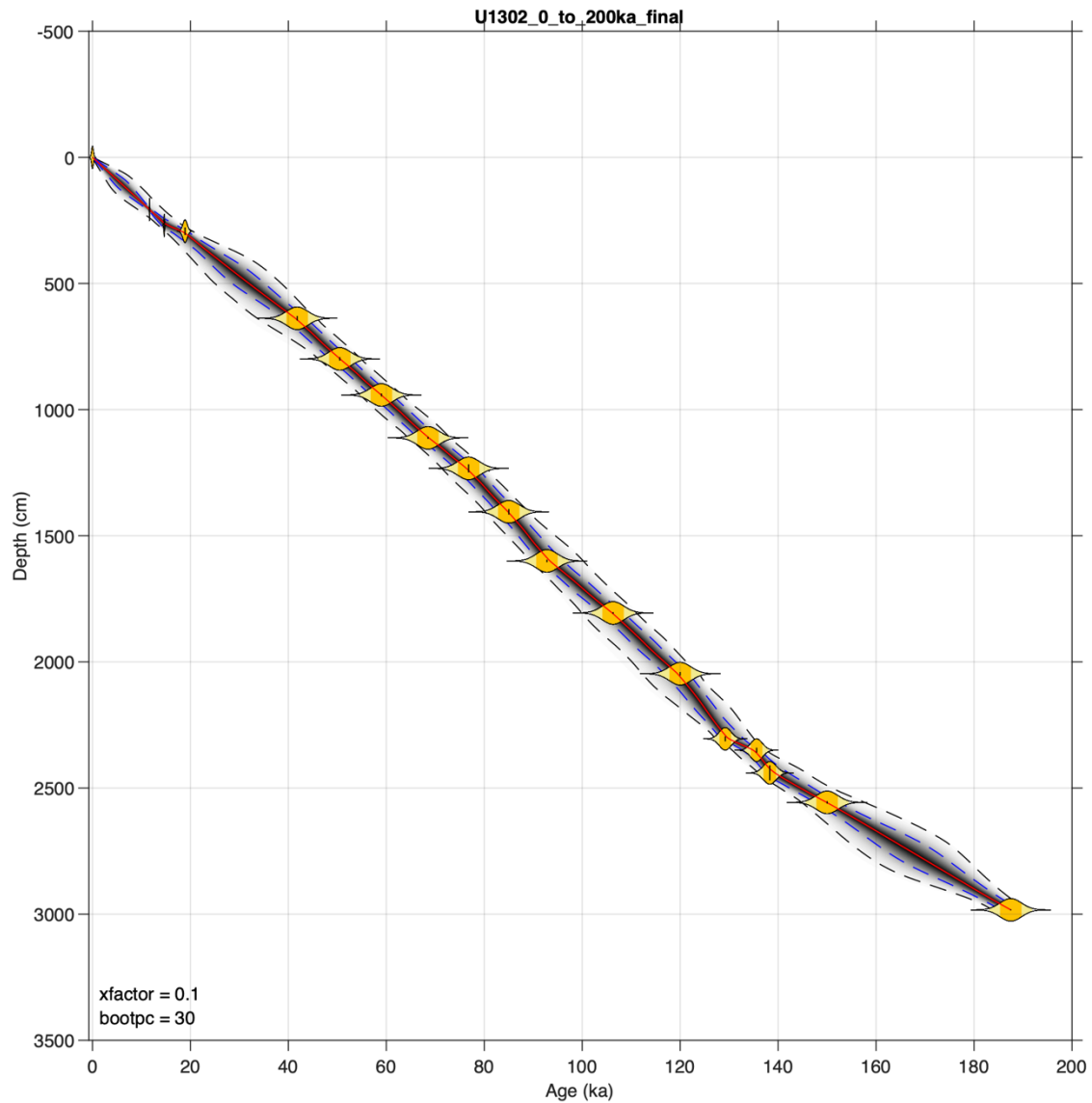


**Figure S1.** Age-depth plot for Site U1302/3 produced by *Undatable* for 0–187 ka. Generated with bootstrapping set to 30% and sedimentation rate uncertainty set to 0.1 (see Lougheed and Obrochta (2019) for details). Yellow probability density functions indicate the radiocarbon and alignment tie points, and tephra age-depth constraints, respectively. The grey cloud indicates the probability density cloud of the age-depth model, whereby darker colours indicate higher age-depth probability. The blue and black broken lines represent 68.27% and 95.45% confidence intervals, respectively. The red line indicates the age-depth model median.

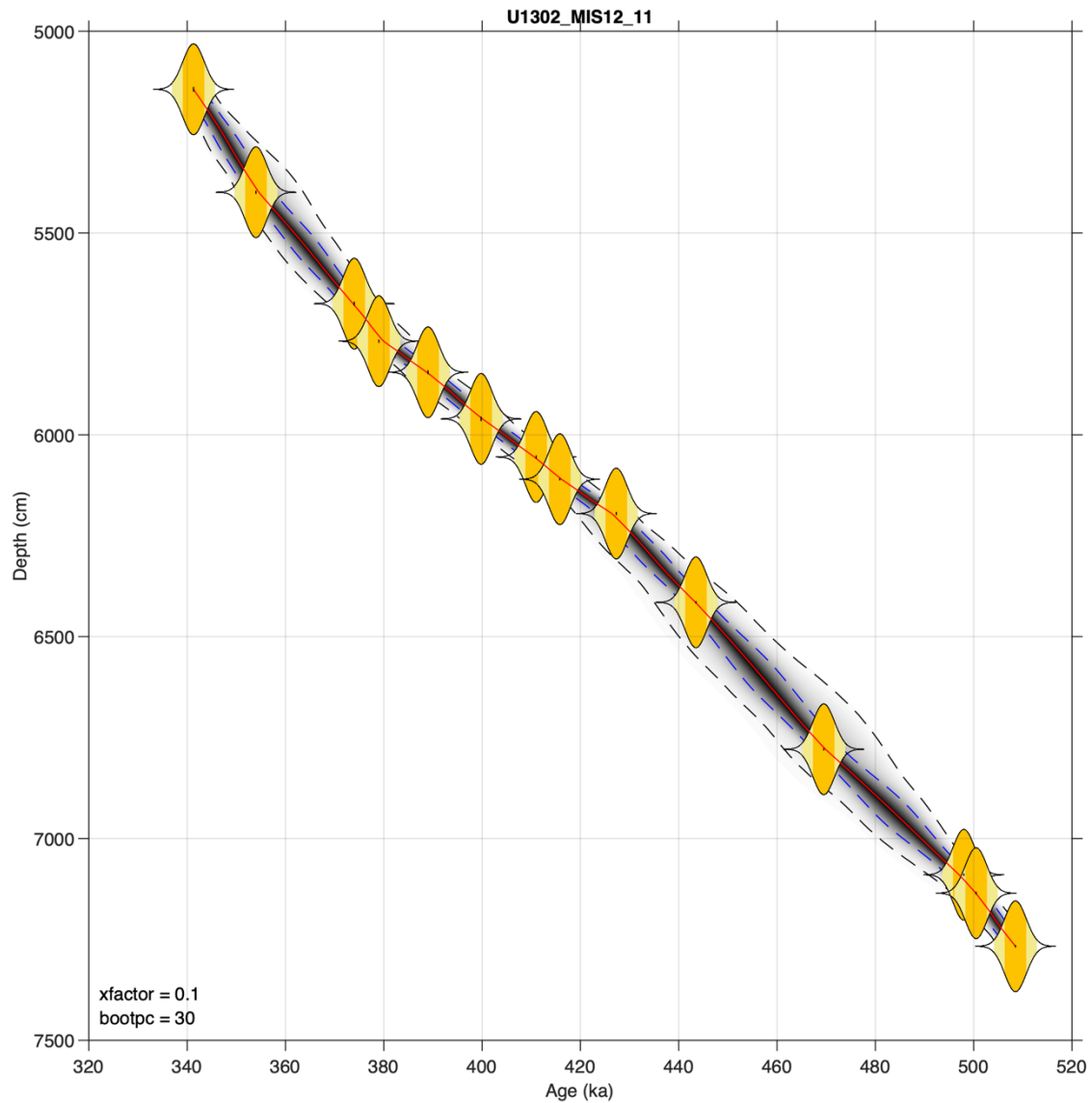


**Figure S2.** Age-depth plot for Site U1302/3 produced by *Undatable* for ~340-508 ka. Generated with bootstrapping set to 30% and sedimentation rate uncertainty set to 0.1 (see Lougheed and Obrochta (2019) for details). Yellow probability density functions indicate the radiocarbon and alignment tie points, and tephra age-depth constraints, respectively. The grey cloud indicates the probability density cloud of the age-depth model, whereby darker colours indicate higher age-depth probability. The blue and black broken lines represent 68.27% and 95.45% confidence intervals, respectively. The red line indicates the age-depth model median.

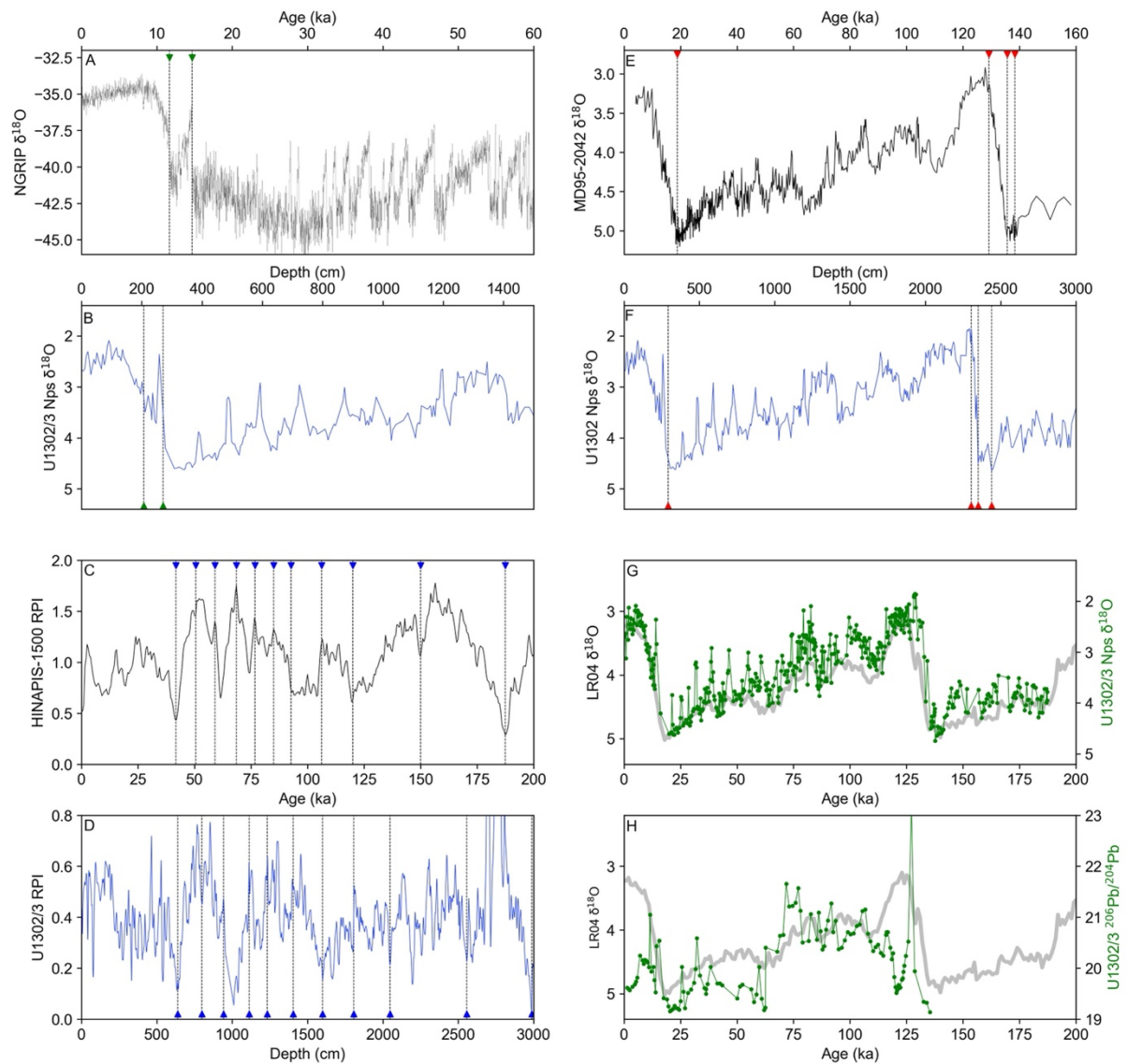


**Figure S3.** Plots that illustrate age-depth tie picks (green, red and blue triangles) used to construct an age model for IODP Site U1302/3 spanning 0–187 ka: **(A)**; Greenland NorthGRIP (NGRIP) ice core air temperature proxy record (Fig. Xa–b; Dansgaard et al., 1982) on the Greenland ice core chronology (GICC05; Rasmussen et al., 2014); **(B)** Site U1302/3 *Neogloboquadrina pachyderma* (l) (Npl)  $\delta^{18}\text{O}$  (Hillaire-Marcel et al., 2011); **(C)** HINAPIS-1500 RPI stack (Xuan et al., 2016); **(D)** Site U1302/3 RPI (Channell et al., 2012); **(E)** Iberian Margin Core MD95-2042 (Shackleton et al., 1995) on Lisiecki and Stern (2016) age model; **(F)** Site U1302/3 Npl  $\delta^{18}\text{O}$ ; **(G)** Site U1302/3 *Neogloboquadrina pachyderma* (l) (Npl)  $\delta^{18}\text{O}$  (green line; Hillaire-Marcel et al., 2011) on the MIS 6–1 age model presented in this study vs. LR04 benthic  $\delta^{18}\text{O}$  stack (thick grey line; Lisiecki and Raymo, 2005); **(H)** Site U1302/3 authigenic  $^{206}\text{Pb}/^{204}\text{Pb}$  (this study) on the MIS 6–1 age model presented in this study vs. LR04 benthic  $\delta^{18}\text{O}$  stack (thick grey line).

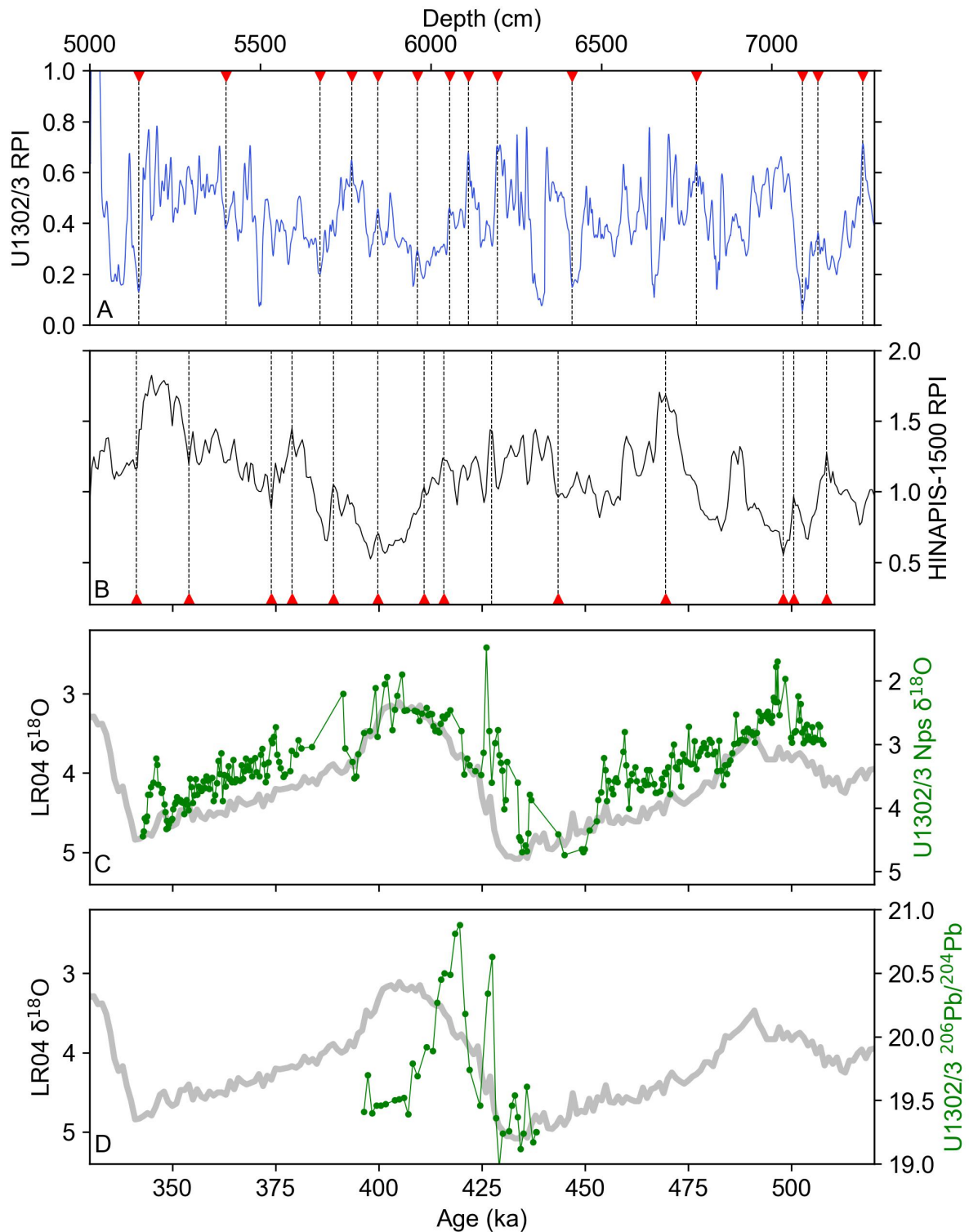


**Figure S4.** Plots that illustrate age-depth tie picks (red triangles) used to construct an age model for IODP Site U1302/3 spanning 341–508 ka: **(A)** Site U1302/3 Relative Paleointensity (RPI) record (Channell et al., 2012); **(B)** HINAPIS-1500 RPI stack (Xuan et al., 2016); **(C)** Site U1302/3 *Neogloboquadrina pachyderma* (l) (Npl)  $\delta^{18}\text{O}$  (green line; Hillaire-Marcel et al., 2011) on the MIS 13–11 age model presented in this study vs. LR04 benthic  $\delta^{18}\text{O}$  stack (thick grey line; Lisiecki and Raymo, 2005); **(D)** Site U1302/3 authigenic  $^{206}\text{Pb}/^{204}\text{Pb}$  (this study) on the MIS 13–11 age model presented in this study vs. LR04 benthic  $\delta^{18}\text{O}$  stack (thick grey line).

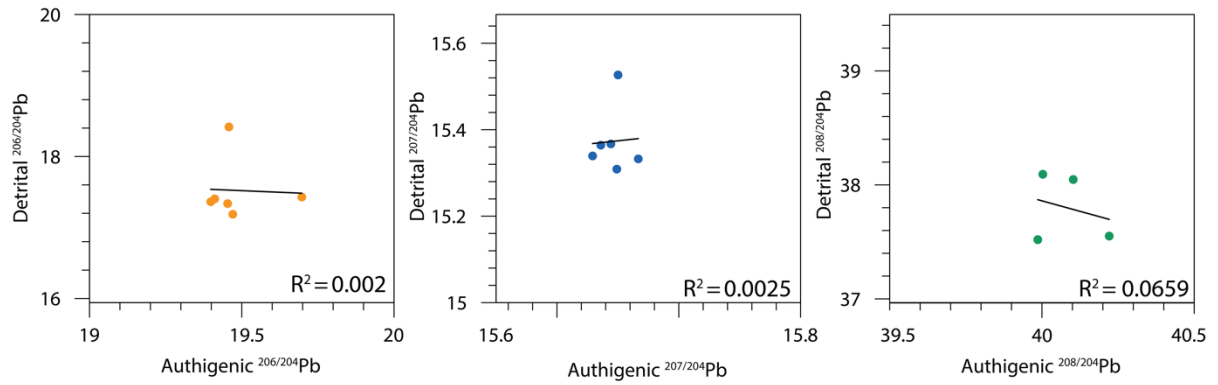


**Figure S5.** Cross plots of paired authigenic and detrital Fe-Mn oxyhydroxide-derived Pb isotope data from IODP Site U1302/3 with regression analysis.

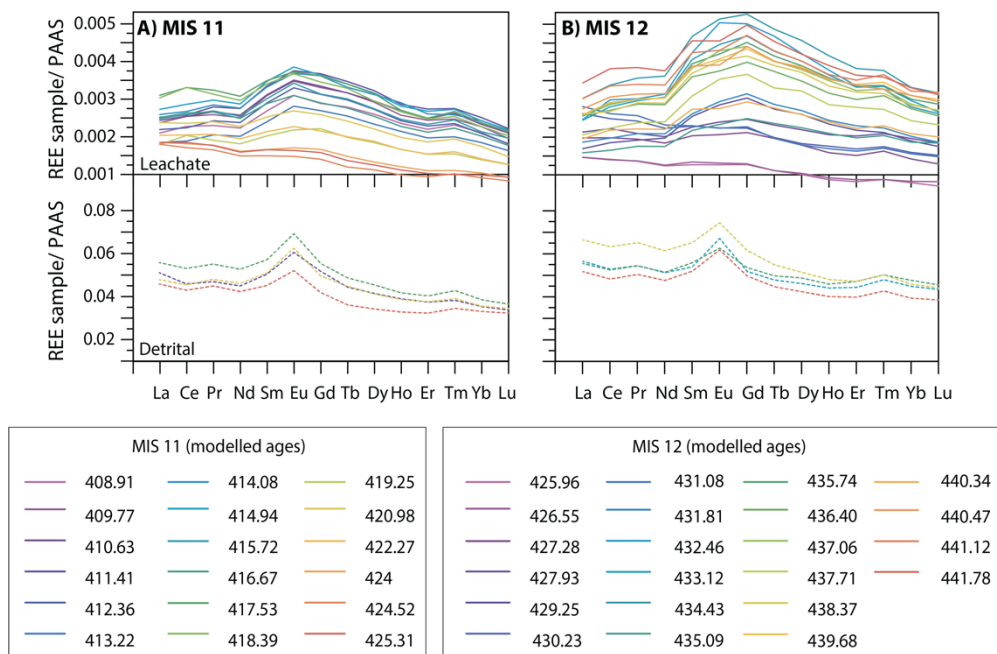


**Figure S6.** Post-Archean Australian Shale (PAAS) normalised rare earth element (REE) multi-element plots for paired authigenic Fe-Mn oxyhydroxide (solid lines) and detrital (dotted lines).

**Table S1.** IODP Site U1302/3 age model: 0–187 ka

Reference chronology (tuning target)					IODP Site U1302/3			
Ref chronostratigraphy	Feature	Placement (mid-pt vs. min/max)	Age and age model uncertainty ( $\pm 1\sigma$ )	Ice core max. count error (ka; $\pm 1\sigma$ )	Mid depth/tie @ (m)	Sediment (half) depth and range over which transition used for tie occurs (in m)	Data used in tuning	Notes
n/a	Core top	n/a	0.0 $\pm$ 0.2 ka		0.00	n/a	n/a	Arbitrary choice of age but has fairly large uncertainty.
NGRIP $\delta^{18}\text{O}$ (GICC05)	Start of Holocene	Mid-point	11.653 (11.703) $\pm$ 0.004	0.050	2.07 $\pm$ 0.10	0.20 (0.10) 1.96–2.16	Planktic $\delta^{18}\text{O}$	Planktic $\delta^{18}\text{O}$ from Hillaire-Marcel et al. (2011)
NGRIP $\delta^{18}\text{O}$ (GICC05)	Start of GI-1e	Mid-point	14.642 (14.692) $\pm$ 0.004	0.093	2.70 $\pm$ 0.25	0.50 (0.25) 2.58–3.08	Planktic $\delta^{18}\text{O}$	Planktic $\delta^{18}\text{O}$ from Hillaire-Marcel et al. (2011)
MD95-2042 $\delta^{18}\text{O}$	MIS 2 maxima	Trough	18.9 $\pm$ 0.45*		2.93 $\pm$ 0.15	0.30 (0.15) 2.78–3.08	Planktic $\delta^{18}\text{O}$	Planktic $\delta^{18}\text{O}$ from Hillaire-Marcel et al. (2011)
HINAPIS-1500 RPI	-	Trough	41.8 $\pm$ 2.2*		6.38 $\pm$ 0.09	0.18 (0.09) 6.29–6.47	RPI	HINAPIS RPI from Xuan et al. (2016)
HINAPIS-1500 RPI	-	Peak	50.5 $\pm$ 2.2*		7.99 $\pm$ 0.07	0.14 (0.07) 7.92–8.06	RPI	HINAPIS RPI from Xuan et al. (2016)
HINAPIS-1500 RPI	-	Peak	59.0 $\pm$ 2.2*		9.42 $\pm$ 0.06	0.12 (0.06) 9.36–9.48	RPI	HINAPIS RPI from Xuan et al. (2016)
HINAPIS-1500 RPI	-	Peak	68.5 $\pm$ 2.2*		11.12 $\pm$ 0.04	0.08 (0.04) 11.08–11.16	RPI	HINAPIS RPI from Xuan et al. (2016)
HINAPIS-1500 RPI	-	Peak	76.8 $\pm$ 2.2*		12.33 $\pm$ 0.16	0.32 (0.16) 12.17–12.49	RPI	HINAPIS RPI from Xuan et al. (2016)
HINAPIS-1500 RPI	-	Peak	85.0 $\pm$ 2.2*		14.05 $\pm$ 0.11	0.22 (0.11) 13.94–14.16	RPI	HINAPIS RPI from Xuan et al. (2016)
HINAPIS-1500 RPI	-	Trough	92.8 $\pm$ 2.2*		16.00 $\pm$ 0.05	0.10 (0.05) 15.95–16.05	RPI	HINAPIS RPI from Xuan et al. (2016)
HINAPIS-1500 RPI	-	Peak	106.3 $\pm$ 2.2*		18.06 $\pm$ 0.03	0.06 (0.03) 18.03–18.09	RPI	HINAPIS RPI from Xuan et al. (2016)
HINAPIS-1500 RPI	-	Trough	120.0 $\pm$ 2.2*		20.47 $\pm$ 0.07	0.14 (0.07) 20.40–20.54	RPI	HINAPIS RPI from Xuan et al. (2016)
MD95-2042 $\delta^{18}\text{O}$		Maxima	129.2 $\pm$ 1.2**		23.05 $\pm$ 0.10	0.20 (0.01) 22.95–23.15	Planktic $\delta^{18}\text{O}$	Planktic $\delta^{18}\text{O}$ from Hillaire-Marcel et al. (2011)
MD95-2042 $\delta^{18}\text{O}$	MIS 6.0	Trough	135.6 $\pm$ 1.2**		23.50 $\pm$ 0.10	0.20 (0.10) 23.4–23.6	Planktic $\delta^{18}\text{O}$	Planktic $\delta^{18}\text{O}$ from Hillaire-Marcel et al. (2011)
MD95-2042 $\delta^{18}\text{O}$	MIS 6.2	Trough	138.3 $\pm$ 1.3**		24.40 $\pm$ 0.30	0.60 (0.30) 24.15–24.75	Planktic $\delta^{18}\text{O}$	Planktic $\delta^{18}\text{O}$ from Hillaire-Marcel et al. (2011)
HINAPIS-1500 RPI	-	Trough	150.0 $\pm$ 2.2**		25.57 $\pm$ 0.05	0.10 (0.05) 25.52–25.62	RPI	HINAPIS RPI from Xuan et al. (2016)
HINAPIS-1500 RPI	-	Trough	187.5 $\pm$ 2.2**		29.88 $\pm$ 0.07	0.14 (0.07) 29.82–29.96	RPI	HINAPIS RPI from Xuan et al. (2016)

\*age uncertainty is propagation of LR04  $1\sigma$  age error (2 ka) and our conservative estimate of depth uncertainty of placing HINAPIS RPI stack on LR04 ages (taken to be 50% of LR04 age error)

\*\*age uncertainty for MD95-2042 from Lisiecki & Stern (2016).

**Table S2.** IODP Site U1302/3 age model: MIS 13–11

Reference chronology (tuning target)			IODP Site U1302/3			
Ref chronostratigraphy	Placement (mid-pt vs.min/max)	Age and age model uncertainty ( $\pm 1\sigma$ )	Mid depth/tie @ (m)	Sediment (half) depth and range over which transition used for tie occurs (in m)	Data used in tuning	Notes
HINAPIS-1500 RPI	Peak	341.3 $\pm$ 2.2	51.44 $\pm$ 0.06	0.12 (0.06) 51.38–51.50	RPI	U1302/3 RPI from Channell et al. (2012). HINAPIS RPI from Xuan et al. (2016).
HINAPIS-1500 RPI	Trough	354.0 $\pm$ 2.2	53.99 $\pm$ 0.04	0.08 (0.04) 53.95–54.03	RPI	U1302/3 RPI from Channell et al. (2012). HINAPIS RPI from Xuan et al. (2016).
HINAPIS-1500 RPI	Peak	374.0 $\pm$ 2.2	56.75 $\pm$ 0.05	0.10 (0.05) 56.70–56.80	RPI	U1302/3 RPI from Channell et al. (2012). HINAPIS RPI from Xuan et al. (2016).
HINAPIS-1500 RPI	Peak	379.0 $\pm$ 2.2	57.68 $\pm$ 0.04	0.08 (0.04) 57.64–57.72	RPI	U1302/3 RPI from Channell et al. (2012). HINAPIS RPI from Xuan et al. (2016).
HINAPIS-1500 RPI	Peak	389.0 $\pm$ 2.2	58.45 $\pm$ 0.05	0.10 (0.05) 58.40–58.50	RPI	U1302/3 RPI from Channell et al. (2012). HINAPIS RPI from Xuan et al. (2016).
HINAPIS-1500 RPI	Peak	399.8 $\pm$ 2.2	59.605 $\pm$ 0.055	0.11 (0.055) 59.55–59.66	RPI	U1302/3 RPI from Channell et al. (2012). HINAPIS RPI from Xuan et al. (2016).
HINAPIS-1500 RPI	Peak	411.0 $\pm$ 2.2	60.55 $\pm$ 0.04	0.08 (0.04) 60.51–60.59	RPI	U1302/3 RPI from Channell et al. (2012). HINAPIS RPI from Xuan et al. (2016).
HINAPIS-1500 RPI	Peak	415.8 $\pm$ 2.2	61.10 $\pm$ 0.03	0.06 (0.03) 61.07–61.13	RPI	U1302/3 RPI from Channell et al. (2012). HINAPIS RPI from Xuan et al. (2016).
HINAPIS-1500 RPI	Peak	427.3 $\pm$ 2.2	61.95 $\pm$ 0.04	0.08 (0.04) 61.91–61.99	RPI	U1302/3 RPI from Channell et al. (2012). HINAPIS RPI from Xuan et al. (2016).
HINAPIS-1500 RPI	Trough	443.5 $\pm$ 2.2	64.15 $\pm$ 0.03	0.06 (0.03) 64.12–64.18	RPI	U1302/3 RPI from Channell et al. (2012). HINAPIS RPI from Xuan et al. (2016).
HINAPIS-1500 RPI	Peak	469.5 $\pm$ 2.2	67.79 $\pm$ 0.03	0.06 (0.03) 67.76–67.82	RPI	U1302/3 RPI from Channell et al. (2012). HINAPIS RPI from Xuan et al. (2016).
HINAPIS-1500 RPI	Peak	498.0 $\pm$ 2.2	70.90 $\pm$ 0.03	0.06 (0.03) 70.87–70.93	RPI	U1302/3 RPI from Channell et al. (2012). HINAPIS RPI from Xuan et al. (2016).
HINAPIS-1500 RPI	Peak	500.5 $\pm$ 2.2	71.355 $\pm$ 0.035	0.07 (0.035) 71.32–71.39	RPI	U1302/3 RPI from Channell et al. (2012). HINAPIS RPI from Xuan et al. (2016).
HINAPIS-1500 RPI	Peak	508.5 $\pm$ 2.2	72.67 $\pm$ 0.03	0.06 (0.03) 72.64–72.70	RPI	U1302/3 RPI from Channell et al. (2012). HINAPIS RPI from Xuan et al. (2016).

\*age uncertainty is propagation of LR04  $1\sigma$  age error (2 ka) and our conservative estimate of depth uncertainty of placing HINAPIS RPI stack on LR04 ages (taken to be 50% of LR04 age error)

### References (not cited in main text)

- Channell, J.E.T., Xuan, C., Hodell, D.A., 2009. Stacking paleointensity and oxygen isotope data for the last 1.5 Myrs (PISO-1500). *Earth Planet. Sci. Lett.* 283, 14–23. <https://doi.org/10.1016/j.epsl.2009.03.012>
- Lisiecki, L. E., and Stern, J. V. (2016), Regional and global benthic  $\delta^{18}\text{O}$  stacks for the last glacial cycle, *Paleoceanography*, 31, 1368–1394. <https://doi.org/10.1002/2016PA003002>
- Rasmussen et al., 2014. A stratigraphic framework for abrupt climatic changes during the Last Glacial period based on three synchronized Greenland ice-core records: refining and extending the INTIMATE event stratigraphy. *Quaternary Science Reviews* 106, 14–28. <https://doi.org/10.1016/j.quascirev.2014.09.007>
- Shackleton, N.J., Hall, M.A., Vincent, E.. 2000. Phase relationships between millennial-scale events 64,000-24,000 years ago. *Paleoceanography* 15(6), 565–569.
- Skinner, L. C., and N. J. Shackleton (2005), An Atlantic lead over Pacific deep-water change across Termination I: Implications for the application of the marine isotope stage stratigraphy, *Quaternary Science Reviews* 24(5–6), 571–580, <https://doi.org/10.1016/j.quascirev.2004.11.008>
- Stern, J. V., and Lisiecki, L. E. (2014), Termination 1 timing in radiocarbon- dated regional benthic  $\delta^{18}\text{O}$  stacks, *Paleoceanography*, 29, 1127–1142. <https://doi.org/10.1002/2014PA002700>